Pergamon

Tetrahedron 58 (2002) 3929–3941

TETRAHEDRON

Investigation of rhodium catalyzed hydroformylation of ethylene in supercritical carbon dioxide by in situ FTIR spectroscopy

Shaker Haji and Can Erkey*

Environmental Engineering Program, Department of Chemical Engineering, University of Connecticut, Storrs, CT 06269-3222, USA

Received 12 November 2001; accepted 5 January 2002

Abstract—The reactions of $RhH(CO)L_3$ ($L=P(3,5\text{-}(CF_3)_2C_6H_3)_3$) with CO, H_2, C_2H_4 and mixtures of these in supercritical carbon dioxide ($scCO_2$) were investigated using high-pressure FTIR spectroscopy. The results were compared to the behavior of the conventional catalyst, $RhH(CO)(PPh_3)_3$, in organic solvents. $RhH(CO)L_3$ does not dissociate in $scCO_2$ and it is converted to $RhH(CO)_2L_2$ and to $[Rh(CO)_2L_2]_2$ in the presence of CO and mainly to $RhH(CO)L_2$ in the presence of an equimolar mixture of CO and H_2. In the presence of CO and C_2H_4, the peaks observed in the acyl region and the terminal metal carbonyl region indicate the formation of three different acylrhodium complexes which are $Rh(CO)L_2(COEt)$, $Rh(CO)_2L_2(COEt)$, and $Rh(CO)_3L(COEt)$. Similar species were also observed during the hydroformylation reaction. The first ever detection of the presence of $Rh(CO)L_2(COEt)$ under hydroformylation conditions provides direct evidence for the mechanism originally proposed by Wilkinson and co-workers. The carbonyl stretching frequencies of all of the rhodium–carbonyl species are shifted to higher wavenumbers due to a reduction of electron density at the metal center by the CF_3 groups.

1. Introduction

As a reaction solvent in homogeneous catalysis, supercritical carbon dioxide ($scCO_2$) offers many advantages over conventional organic solvents.[1,2]

1. Many gases exhibit higher solubilities in $scCO_2$ than in organic solvents.[3] Thus, based simply on increased concentration of reactants, faster reactions are expected to occur within the $scCO_2$ phase provided that the reaction order with respect to the gaseous substrate is positive.
2. Conducting the reaction in a single phase can eliminate the problems when mass transfer controls the reaction rate across the gas–liquid interface.
3. The design, scale-up and operation of reactors operating in single phase are much simpler than multiphase reactors.
4. The unusual solvent properties of $scCO_2$ may lead to increased rates or selectivities due to solvent effects in homogeneous catalysis. Transition metal complexes in catalytic cycles participate only in a few types of reactions such as ligand exchange, insertion, oxidative addition and reductive elimination. The overall rate of the reaction and in some cases the selectivity depend on the equilibria between the reactive intermediates in solution, which is influenced by the nature of the solvent. Using $scCO_2$ may shift such equilibria in the desired direction.
5. $scCO_2$ is non-flammable, non-toxic, environmentally acceptable, cheap, readily available in large quantities and has a low critical temperature and a moderate critical pressure.
6. The strong dependency of the solubility of solutes in $scCO_2$ to temperature and pressure in the vicinity of the critical point may be exploited in development of efficient catalyst separation/recovery and product purification schemes.

Although $scCO_2$ has very attractive properties as a reaction medium in homogeneous catalysis, the low solubility of conventional homogeneous catalysts in $scCO_2$ has hindered developments in this area.[4] One way to increase solubility in $scCO_2$ is to utilize CO_2-philic moieties such as fluoroether, fluoroalkyl, fluoroacrylate, siloxane, or phosphazene. In the pioneering example on developing chelating agents for $scCO_2$ extraction of heavy metals from aqueous solutions, fluorination of the ethyl groups of the diethyldithiocarbamate (DDC) ligand was found to enhance the solubilities of $Cu(DDC)_2$, $Ni(DDC)_2$, and $Co(DDC)_3$ in $scCO_2$ by three orders of magnitude.[5] This discovery has been one of the key developments in $scCO_2$ research. Subsequently, a wide variety of reagents functionalized with CO_2-philic groups were developed for $scCO_2$ applications.[6,7]

During the past 3 years, significant advances have also been made in development of synthetic methods for

Keywords: in situ FTIR; hydroformylation; rhodium; supercritical carbon dioxide; fluorinated phosphines; homogeneous catalysis.

* Corresponding author. Tel.: +1-860-486-4601; fax: +1-860-486-2959; e-mail: cerkey@engr.uconn.edu

0040–4020/02/$ - see front matter
PII: S0040-4020(02)00246-6

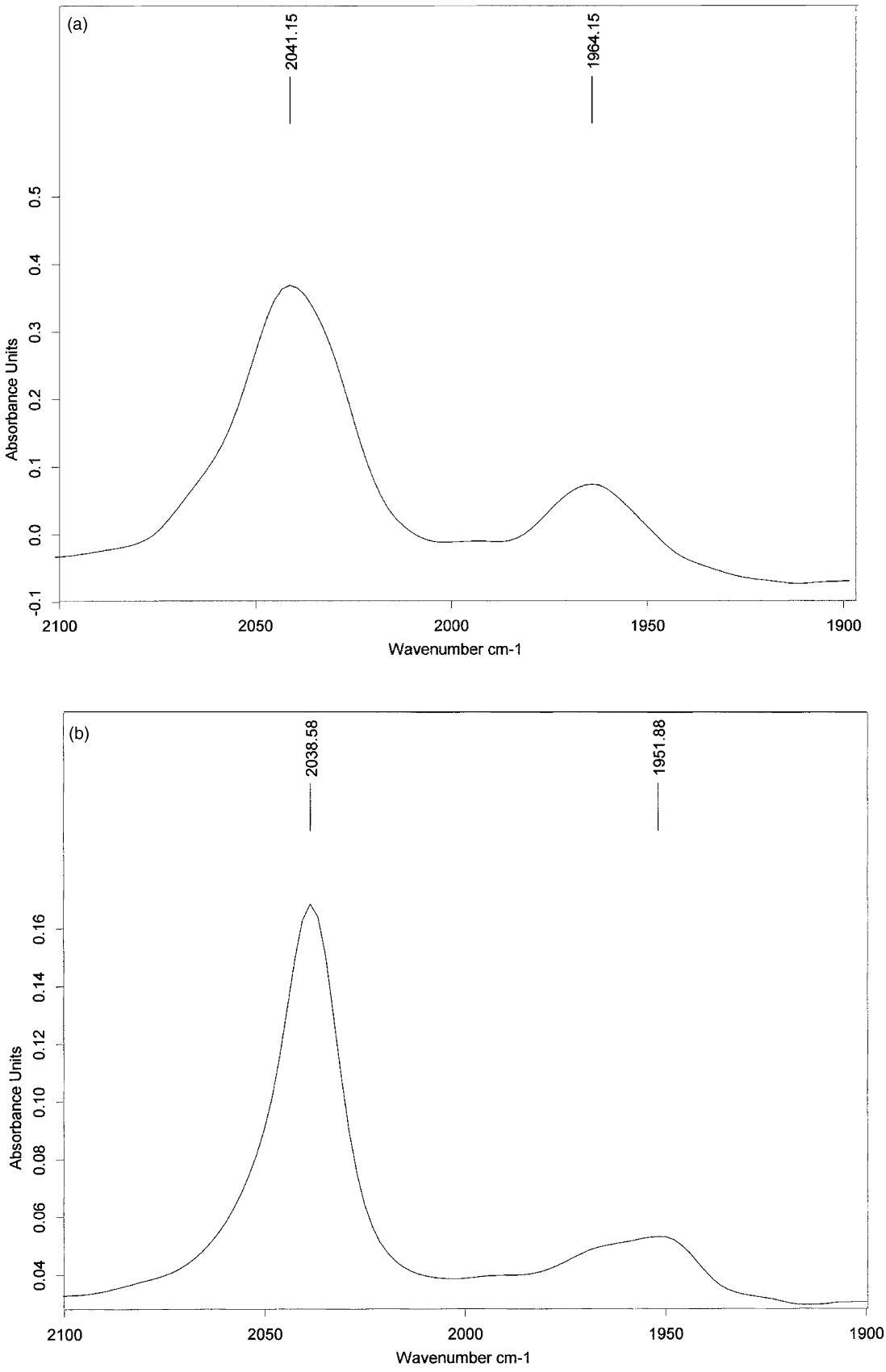

Figure 1. Spectra of **1**: (a) in $scCO_2$ at 50°C and 115 bar (3 mM), and (b) in solid form.

homogeneous catalysts, which exhibit high solubilities in $scCO_2$. These started with the pioneering work of Kainz and Leitner who prepared triarylphosphine ligands with perfluoroalkyl tails.[8] The rhodium complexes of these ligands were found to be sufficiently soluble in $scCO_2$ and could catalyze the hydroformylation of olefins. Along the same time period, an interesting coincidence and an important development was the invention of fluorous biphasic systems (FBS) by Horvath and Rabei[9] as a means to tackle the problems associated with catalyst recovery/recycle in homogeneous catalysis. The success of this approach depends on favorable partitioning of fluorous homogeneous catalysts into the fluorous phase. Subsequently, quite a few studies appeared in the literature on synthesis, characterization and reactive properties of fluorinated ligands, primarily phosphines.[10–14] Our group synthesized and characterized several fluoroalkyl and fluoroalkoxy substituted tertiary aryl phosphine ligands {$[3,5\text{-}(CF_3)_2C_6H_3]_3P$, $(4\text{-}CF_3C_6H_4)_3P$, $(3\text{-}CF_3C_6H_4)_3P$, $(4\text{-}CF_3OC_6H_4)_3P$, $[4\text{-}F(CF_2)_4(CH_2)_3C_6H_4]_3P$]} and rhodium complexes of some of these ligands ($HRhCOL_3$) as hydroformylation catalysts.[15,16] Organometallic complexes of similar CO_2-philic phosphine ligands were found to efficiently catalyze other types of reactions such as enantioselective hydrogenation,[17] hydrovinylation[18] and hydroformylation[19] in $scCO_2$.

An important consideration in incorporation of fluorous groups into conventional ligands is the effect of electron withdrawing nature of flurous groups on activity and selectivity. For example, in hydroformylation in $scCO_2$, the activity of the catalyst formed in situ from $Rh(CO)_2(ACAC)$ and $[3,5\text{-}(CF_3)_2C_6H_3]_3P$ (**2**) as ligand, was higher by a factor of 5 than that when the ligand was $[4\text{-}F(CF_2)_4(CH_2)_3C_6H_4]_3P$.[20] Likewise, perfluoroalkyl substituted BINAPHOS resulted in higher regioselectivities compared to the unsubstituted ligand in enantioselective hydroformylation in organic solvents.[19] Our primary objective in this study is to probe the effects of fluorous groups on the nature and distribution of intermediates in $scCO_2$ by in situ FTIR spectroscopy for a reaction that is reasonably well understood, namely hydroformylation of olefins by rhodium/phosphine complexes. In situ FTIR spectroscopy is a powerful tool well suited particularly for such investigations since the intermediates can be identified and monitored at catalytic concentrations under reaction conditions.

Hydroformylation of olefins catalyzed by hydridocarbonyltris(triphenylphosphine)rhodium (I), $RhH(CO)(PPh_3)_3$ (**3**), has been extensively studied by a wide variety of techniques including FTIR spectroscopy by Wilkinson and his co-workers[21–24] and by Morris and Tinker.[25] In the late eighties, development of mid-range infrared optical fibers enabled the measurements to be carried out in situ at high temperatures and pressures.[26] The studies by Moser et al. using Cylindrical Internal Reflectance FTIR (CIR/FTIR) at extended temperatures and pressures improved our understanding of the underlying mechanism of the hydroformylation reaction.[27,28] Even though, in situ FTIR spectroscopy has been used for probing homogeneous chemical reactions in supercritical fluids,[29] no studies in the literature has been reported on spectroscopic identification of reactive intermediates in $scCO_2$ solutions with ligands substituted with fluorous groups. In this article, we report the results of our investigations of reactions of hydridocarbonyltris(3,5-bis-(trifluoromethyl)phenylphosphine)rhodium (I), $RhH(CO)\text{-}[P(3,5\text{-}(CF_3)_2C_6H_3)_3]_3$ (**1**), with CO, H_2, and ethylene in dense CO_2 using a high-temperature high-pressure transmission FTIR probe. Ethylene was selected as the substrate to simplify interpretation of the spectra. The results were compared to the behavior of the conventional catalyst **3** in organic solvents.

2. Results and discussion

The concentration of **1** ranged from 2 to 3 mM in all experiments to achieve a satisfactory signal-to-noise ratio.

2.1. The nature of 1 in carbon dioxide

350 mg (3 mM) of $HRh(CO)L_3$ (**1**) was placed in the vessel. The vessel first was heated to 50°C and then was pressurized with CO_2 up to 115 bar bringing the solvent to supercritical conditions. The solution became yellow immediately with complete dissolution of **1**. The spectra were taken every 5 min for 30 min. There were no changes in the successive spectra and the spectra after 30 min is shown in Fig. 1a. The bands at 2041 and 1964 cm^{-1} were assigned to the metal hydride (νRhH) and the carbonyl (νCO) in **1**, respectively. The spectra of **1** in solid form is shown in Fig. 1b (νRhH=2039 cm^{-1} and νCO=1952 cm^{-1}). The ν(CO) is a sensitive indicator of electron density at the metal center, yielding a relative measure of the amount of π-backbonding from an occupied metal d-orbital to the empty π^*-orbital of the carbonyl. Comparison of νCO of **1** with that of the conventional catalyst **3** (1952 vs 1923 cm^{-1}, solid spectra)[21] reveals that metal–carbonyl bond is weaker in **1** compared to **3** which is due to a reduction of electron density at the metal center caused by the electron withdrawing CF_3 groups. The first possibility is that electron density reduction is caused by a strong electron back donation to the fluorinated ligand **2** if it is σ-donor/π-acceptor. The second possibility is that the electron density reduction is due to less electron donation from **2** compared to triphenylphosphine to the metal center. This would be true if **2** is pure σ-donor.

The similarity of the spectra of **1** in solid form and in solution indicates that **1** does not dissociate in $scCO_2$. The slight shift in νCO in solution indicates the effect of the solvent on the electronic structure of **1**. The NMR spectra of **1** in acetone-d_6 shows that **1** does not dissociate in acetone also. Both ^1H NMR and $^{31}P\{^1H\}$ NMR showed no evidence of any band or broad band near the frequencies of the pure ligand **2**. This behavior is markedly different from the behavior of the conventional catalyst **3**, which was found to undergo ligand dissociation in solvents such as benzene, dichloromethane, and cyclohexane. Evans and co-workers[21] suggested the following equilibria based on molecular weights measured by osmometric techniques:

$$RhH(CO)(PPh_3)_3 \underset{+PPh_3}{\overset{-PPh_3}{\rightleftharpoons}} RhH(CO)(PPh_3)_2 \underset{+PPh_3}{\overset{-PPh_3}{\rightleftharpoons}} RhH(CO)(PPh_3) \quad (1)$$

They also reported an appreciable difference in the metal

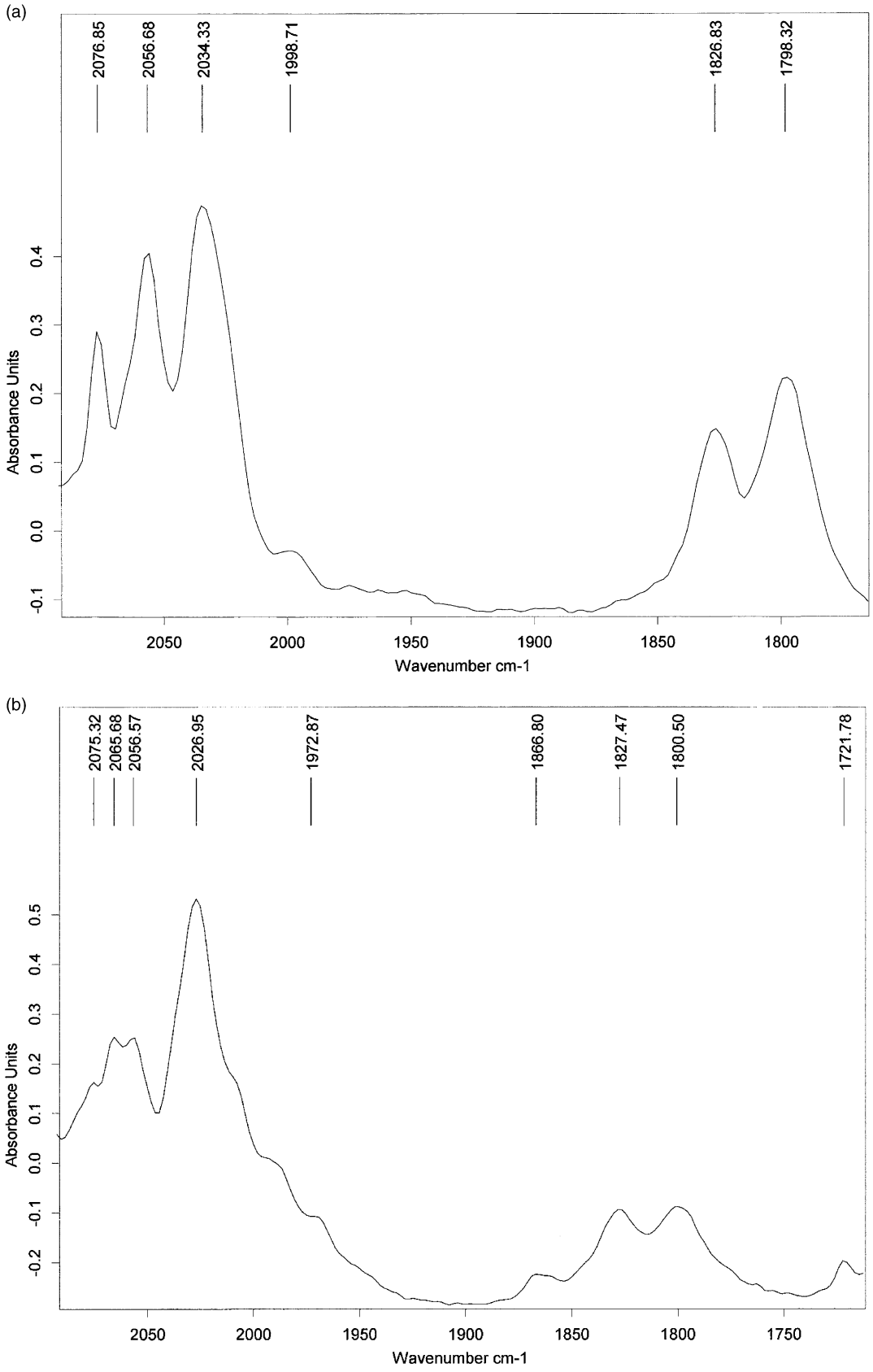

Figure 2. (a) Spectra of **1** (2.73 mM) in $scCO_2$ at 50°C and 115 bar with CO (165 mM), and (b) after the addition of H_2.

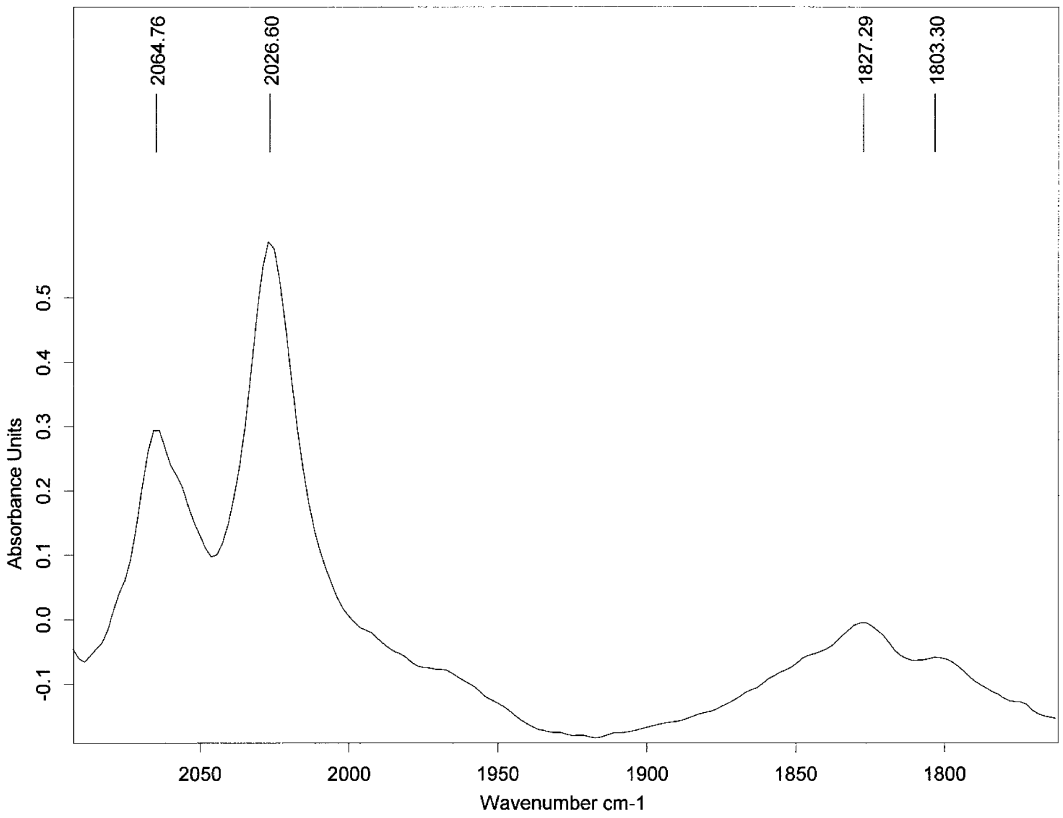

Figure 3. Spectra of **1** (2.73 mM) in $scCO_2$ at 50°C and 115 bar with 1:1 mixture of CO/H_2 (150 mM each).

hydride stretching frequency in IR spectra of **3** in solution and in solid form which is not the case observed with **1**. Such behavior is indicative of a stronger metal–ligand bond in **1** than in the conventional catalyst due to trifluoromethyl groups.

2.2. Reaction of 1 with carbon monoxide in carbon dioxide

300 mg (2.73 mM) of **1** was placed in the vessel. After the vessel was heated to 50°C and flushed with CO, it was pressurized with CO to 4.5 bar (165 mM) and then pressurized with CO_2 up to 115 bar. The mixture became a single phase in a few minutes with complete dissolution of **1**. While filling the reactor with CO_2, the solution color rapidly changed from yellow to dark orange to finally dark red. The IR spectrum is shown in Fig. 2a. One of the new formed complexes is expected to be the hidrydodicarbonylmetal complex, $RhH(CO)_2L_2$ (**5**), for two reasons; the appearance of three bands and the appearance of two of those bands at the terminal M–CO region. The metal hydride frequency appeared at 2076 cm^{-1} while the two carbonyl-stretching frequencies were at 2056 and 2034 cm^{-1}. The ν(CO) of **5** are higher than the ν(CO) of $RhH(CO)_2(PPh_3)_2$ (1980 and 1939 cm^{-1})[21] due to a reduction of electron density at the metal center. Such an increase in ν(CO) with decreasing basicity of the ligand was also observed by Moser et al. for $RhH(CO)_2(P(p\text{-}Z\text{-}C_6H_4)_3)_2$ where Z is $N(CH_3)_2$, OCH_3, H, F, Cl, or CF_3.[27] When Z was CF_3, the frequencies were 2050, 1997, and 1953 cm^{-1}. Therefore, the existence of a second CF_3 group results in a very significant shift to a higher wavenumber. Furthermore, the smaller electron density on the metal results in more electron donation from H^- and a stronger metal hydride bond. The solvent could also have some effect on these shifts. The IR spectrum in Fig. 2a also indicates the presence of an appreciable amount of the dimer, $[RhH(CO)_2L_2]_2$ (**6**); two bands of this species are clearly seen at 1827 and 1799 cm^{-1} and were assigned to the bridging carbonyl groups. The analogous dimer reported previously[21,27] are reported to have four bands, two in the carbonyl-bridging region and the other two in the terminal carbonyl region. In this case, the terminal carbonyl could not be observed since the three strong bands of $RhH(CO)_2L_2$ (**5**) might be obscuring them.

The results indicate that in the presence of CO, **1** undergoes ligand dissociation in solution based on the following equilibria:

$$RhH(CO)L_3 \underset{+L}{\overset{-L}{\rightleftharpoons}} RhH(CO)L_2 \underset{-CO}{\overset{+CO}{\rightleftharpoons}} RhH(CO)_2L_2 \underset{+H_2}{\overset{-H_2}{\rightleftharpoons}} [Rh(CO)_2L_2]_2 \quad (2)$$

and the equilibria in the first two reactions in Eq. (2) are shifted way to the right in the presence of excess CO.

When hydrogen was added to the solution, the spectrum in Fig. 2b showed the emergence of new bands and weakening of others. Two of those new bands were assigned to $RhH(CO)L_2$ (**4**) (νRhH=2066 cm^{-1} and νCO=2027 cm^{-1}). The amounts of both the dicarbonyl complex **5** and the dimer **6** were reduced appreciably, which provides

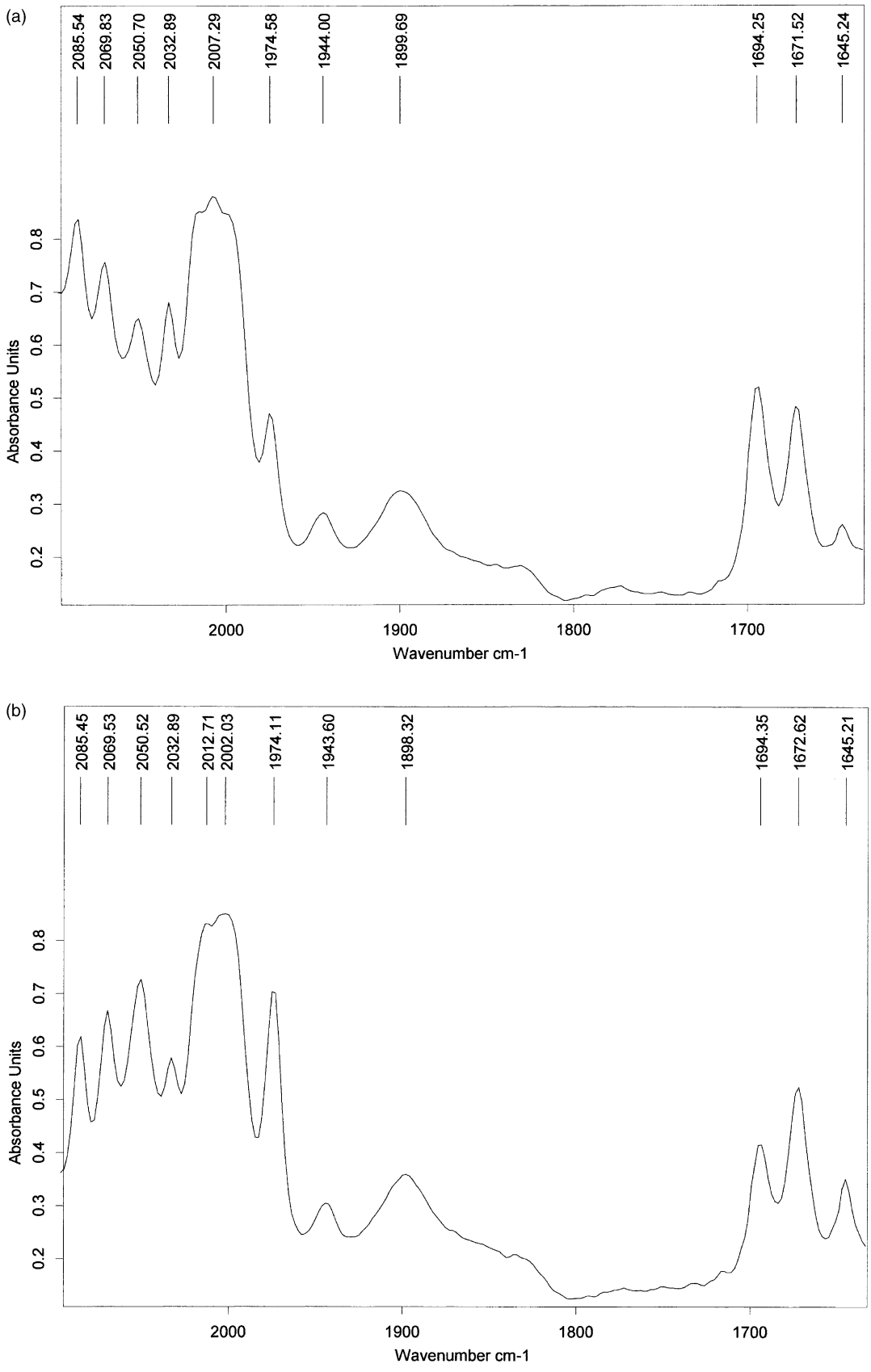

Figure 4. The spectra of **1** (2.2 mM) in liquid CO_2 at 1.5°C and 40 bar in different CO/C_2H_4 mole ratios (those spectra were not subtracted from the solvent–carbon monoxide solution, the peaks at 1944 and 2070 cm^{-1} are solvent peaks): (a) with CO/C_2H_4=1 (140 mM each); (b) with CO/C_2H_4=0.35 (50 mM CO and 140 mM ethylene); and (c) with CO/C_2H_4=0.035 (10 mM CO and 285 mM ethylene).

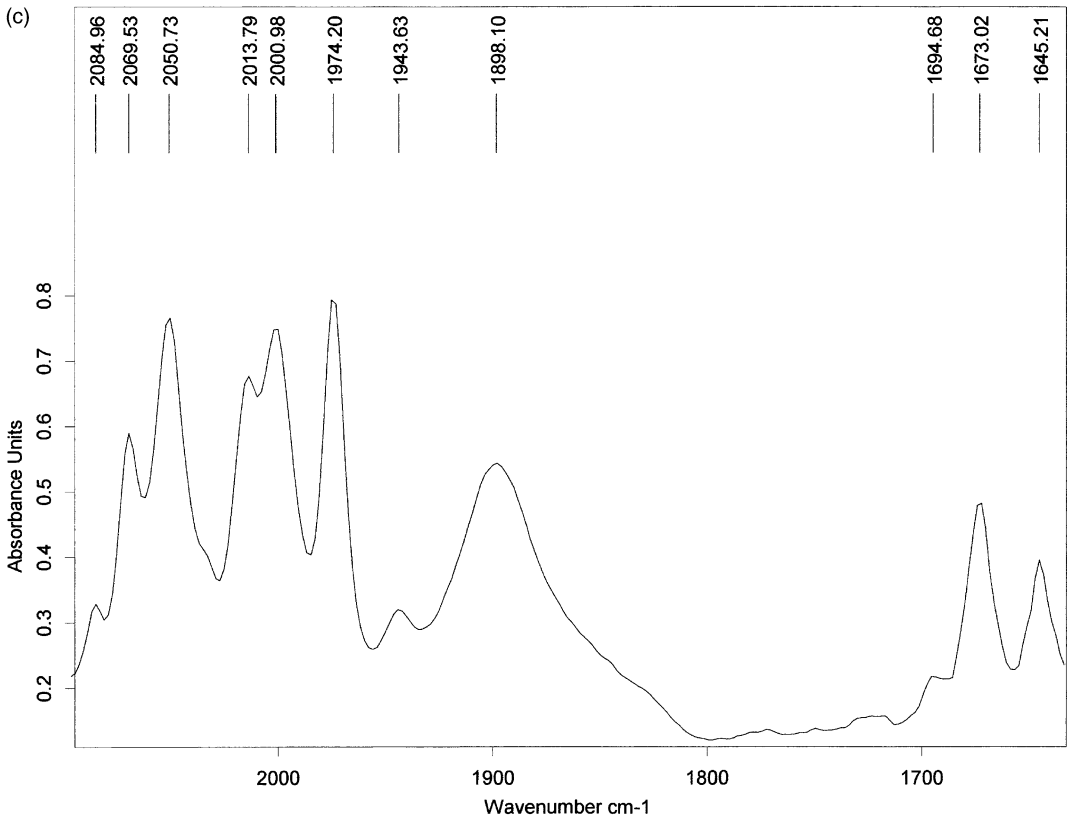

Figure 4. (*continued*)

further proof of the existence of the equilibrium in Eq. (2). The lowest band assigned to **5** (2034 cm^{-1}) could not be detected because it was probably obscured by the strong band of **4** (2027 cm^{-1}). Three other shoulders at 2012, 1996, and 1973 cm^{-1} and another weak peak at 1867 cm^{-1} could not be assigned to any complex. The color of the solution remained dark red throughout the experiment.

2.3. Reaction of 1 with carbon monoxide/hydrogen in carbon dioxide

This experiment is similar to the one above, except that the hydrogen was added at the same time with CO at a 1:1 ratio. The reaction was carried out at 50°C with 300 mg of **1** (2.73 mM), 8 bar of 1:1 CO/H_2 mixture (150 mM each) and the rest CO_2 to make the total pressure of the system 115 bar. The yellow powder **1** dissolved immediately. The CO/H_2 mixture dissolved after a few minutes resulting in a single-phase dark yellow solution. The spectra were taken every 10 min for four times. There were no changes in the successive spectra and the spectra after 30 min is shown in Fig. 3. Two distinguished bands are seen clearly at 2065 and 2027 cm^{-1}, which were assigned to the metal hydride (νRhH) and the carbonyl (νCO) of **4**, respectively. Since the bands of **1** were not detected, the equilibrium for the first reaction in Eq. (2) is shifted away to the right. Although the catalyst undergoes ligand dissociation in the presence of CO/H_2, the presence of hydrogen inhibited CO coordination to the dissociated catalyst **4**. The very weak bands observed at 1827 and 1803 cm^{-1} were assigned to the dimer **6** which should be in equilibrium with a small amount of dicarbonyl complex **5** as can be seen upon close inspection of Fig. 3. In case of the conventional catalyst the analog of complex **4** was observed by Evans and co-worker[21] to absorb at 2000 and 1920 cm^{-1} in dichloromethane, however, that species was observed when 3 was dissolved in a solvent. Moser et al.[27] found no evidence of the analog of **4** under hydroformylation conditions with the conventional catalyst system. In studies of hydroformylation of 1-hexene by $RhH(CO)(PPh_3)_3$ (**3**) using an in situ high-pressure $^{31}P\{^1H\}$ NMR probe,[30] the analog of **4** could not be detected. The existence of **4** in $scCO_2$ shows that the equilibrium composition for the reactions given in Eq. (2) are strongly affected by the CF_3 groups and also perhaps by the solvent. Since the color of the solution in this experiment was dark yellow, the red color solution in the previous experiment could have been caused by either the dicarbonyl complex **5** or the dimer **6**. At the end of the experiment, the reaction mixture was cooled, depressurized, and NMR spectra were taken for the solid. ^1H NMR and $^{31}P\{^1H\}$ NMR spectra showed peaks for the free ligand, in case of $^{31}P\{^1H\}$ NMR the peak was broad. In addition, ^1H NMR and $^{31}P\{^1H\}$ NMR showed that most of **4** reverts back to **1** after the removal of CO/H_2 and the solvent.

2.4. Reaction of 1 with carbon monoxide and ethylene in carbon dioxide

240 mg (2.2 mM) of **1** was charged into the reactor. At 1.5°C, the reactor was pressurized with ethylene up to 3.15 bar (140 mM) then with CO up to 6.3 bar (140 mM) and finally with CO_2 up to 42 bar ($CO/Rh=64$, $CO/C_2H_4=1:1$). The solution was initially two phases with a yellow

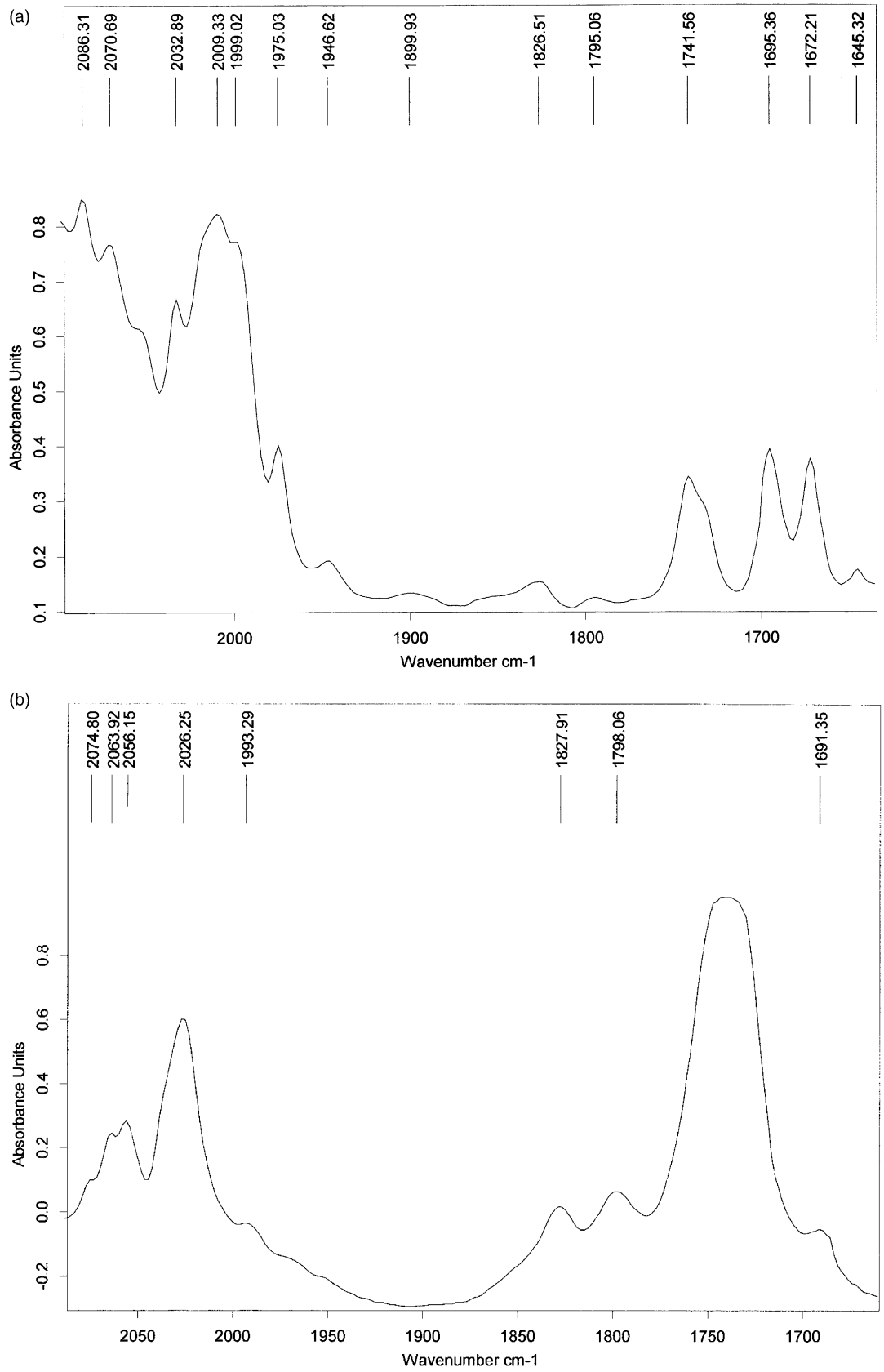

Figure 5. (a) Spectra of the hydroformylation of ethylene (63 mM) in CO_2 (14°C, 65 bar) with 1:1 mixture of CO/H_2 (240 mM each) catalyzed by **1** (2.73 mM) (peaks at 1944 and 2070 cm^{-1} are solvent peaks); and (b) The spectra at the end of the hydroformylation reaction at 50°C and 200 bar.

catalyst-rich bottom phase. The IR spectra of the bottom phase were acquired at this temperature every 2.5 min for 15 min. Subsequently, the vessel was heated to 50°C. All the spectra had similar peaks, but the intensities decreased slightly with increasing temperature. While heating, the system turned into one phase at 24°C. With further heating to 50°C, the pressure increased up to 162 bar. The solution color stayed the same throughout the entire period of heating. The spectrum at 1.5°C and 42 bar is shown in Fig. 4a which shows that **1** is converted to different species. Three peaks appeared in the acyl frequency range and another seven peaks in the terminal metal carbonyl range. The effect of decreasing CO concentration is shown in Fig. 4b (CO/C_2H_4=0.35, 50 mM of CO and 140 mM of ethylene) and Fig. 4c (CO/C_2H_4=0.035, 10 mM of CO and 285 mM of ethylene). Comparing Fig. 4a–c, it was concluded that since the intensities of the three peaks in the acyl frequency range changed with CO/C_2H_4 mole ratio, they were for three different acylrhodium species. When the ratio of CO/C_2H_4 charged to the reactor was reduced, the intensity of the first acyl peak (1645 cm^{-1}) increased along with the peak at 1975 cm^{-1}, while that of the third acyl peak (1695 cm^{-1}) decreased along with the peak at 2086 cm^{-1} and both peaks at 2008 and 2033 cm^{-1} disappeared. The intensity of the middle acyl peak (1673 cm^{-1}) changed slightly. This behavior indicates that the three species are mono-, di-, and tricarbonyl acylrhodium complexes. The bands at 1645 and 1975 cm^{-1} were assigned to the carbonyl in the acyl group and the terminal metal carbonyl, respectively, in the monocarbonyl acylrhodium intermediate, $Rh(CO)L_2(COEt)$ (**7**). The band at 1673 cm^{-1} and the two bands at 2014 and 2051 cm^{-1} were assigned to the carbonyl in the acyl group and the two terminal metal carbonyls, respectively, in the dicarbonyl acylrhodium intermediate, $Rh(CO)_2L_2(COEt)$ (**8**). The band at 1695 cm^{-1} and the three bands at 2008, 2033, and 2086 cm^{-1} were assigned to the carbonyl in the acyl group and the three terminal metal carbonyls, respectively, in the tricarbonyl acylrhodium intermediate, $Rh(CO)_3L(COEt)$ (**9**). The presence of CO more likely converted **1** to **4**, which further reacted with ethylene to form many different species. A plausible pathway is given below:

$$\begin{aligned} RhH(CO)L_3 &\overset{-L}{\underset{+L}{\rightleftharpoons}} RhH(CO)L_2 \overset{+C_2H_4}{\underset{-C_2H_4}{\rightleftharpoons}} RhH(CO)L_2(C_2H_4) \\ &\rightleftharpoons Rh(CO)L_2(Et) \overset{+CO}{\underset{-CO}{\rightleftharpoons}} Rh(CO)_2L_2(Et) \\ &\rightleftharpoons Rh(CO)L_2(COEt) \overset{+CO}{\underset{-CO}{\rightleftharpoons}} Rh(CO)_2L_2(COEt) \\ &\overset{+CO/-L}{\underset{-CO/+L}{\rightleftharpoons}} Rh(CO)_3L(COEt) \end{aligned} \quad (3)$$

Among the three acyl species, analogues of **7** and **9** were not detected before in conventional hydroformylation studies. The band at 2001 cm^{-1} seen in Fig. 4a, was noticed to appear in wide range of frequencies in different experiments with different CO/C_2H_4 ratios, from 1997 to 2002 cm^{-1}. Since the intensity of the peak was not changing with CO/C_2H_4 ratio, it was not assigned to any acylrhodium species. The broad band observed at 1899 cm^{-1} is one of the bands of ethylene. The peaks at 1944 and 2070 cm^{-1} are solvent peaks. It is also worth mentioning that when only ethylene is charged to the reactor, no peaks were observed in the 1620–1700 cm^{-1} region.

2.5. Hydroformylation reaction of ethylene with 1 in carbon dioxide

The preliminary experiments conducted at 50°C indicated that the ethylene hydroformylation reaction was very fast to follow the intermediates. Therefore, the reaction was carried out at 14°C and 65 bar in liquid CO_2 with 300 mg of **1** (2.73 mM), 11.5 bar of 1:1 CO/H_2 mixture (240 mM each) and 1.5 bar ethylene (63 mM). The reaction mixture was initially two phases with a yellow catalyst-rich bottom phase. As usual, **1** dissolved immediately. IR spectra of the homogeneous bottom phase were acquired every 2.5 min for 10 min. The consecutive spectra showed no changes in the reaction mixture species and the spectra at the end of 10 min is shown in Fig. 5a (the spectra is not subtracted from solvent–CO solution, peaks at 1947 and 2071 cm^{-1} are due to the solvent). The peak at 1741 cm^{-1} was assigned to the carbonyl group of propionaldehyde, based on the spectrum of propionaldehyde in CO_2 at the same conditions, indicating small conversion. Weak bands of ethylene also were observed (for example peak around 3100 cm^{-1} and a hump at around 1899 cm^{-1}), indicating some unconverted ethylene. As in the previous set of experiments, all of the peaks in the 1975–2086 cm^{-1} region were visible (1975, 1999, 2009, 2014, 2033, 2051, and 2086 cm^{-1}), as well as the peaks assigned to the acyl groups of **7**, **8**, and **9** (1645, 1672, and 1695 cm^{-1}). The dimer **6** also appeared in very low concentration, however, the band at 1799 cm^{-1} was shifted to 1795 cm^{-1}. Then the heating was started while the data acquisition continued. While heating, the intensities of propionaldehyde peaks (1741, 2989, 2951, 2906, 2821, and 2724 cm^{-1}) increased, especially when the solution turned into one phase at 27°C and 81 bar. At the same time the acylrhodium complexes' peaks were decreasing in intensities slowly. Changes were also noticed in the 1900–2100 region. The color started to change to dark orange and then to dark red at the end of the reaction. The reaction stopped when all the ethylene was consumed. The intensity of the propionaldehyde peaks stopped increasing and leveled off and the three acylrhodium peaks disappeared. The spectra at the end of the reaction at 50°C and 200 bar is shown in Fig. 5b. The following species were observed: propionaldehyde with a peak at 1741 cm^{-1}, the dimer **6** with peaks at 1798 and 1828 cm^{-1}, the species, $RhH(CO)L_2$ (**4**), with peaks at 2026 and 2064 cm^{-1}, and finally the hydridodicarbonyl complex **5** with two of its peaks at 2075 and 2056 cm^{-1}. A weak band was observed at 1993 cm^{-1} but could not be related to any species. After the completion of the hydroformylation reaction and under the presence of extra CO/H_2, the major species in the reaction mixture are **4** and **5**. Subsequently, the reaction mixture was cooled, depressurized and the recovered solid residue was analyzed by NMR. The $^{31}P\{^1H\}$ NMR showed the presence of **1** as a major species, which indicates that during the removal of CO/H_2, **5** was converted to **4** which reassociated with the free ligand **2** to form **1** in accordance with the equilibria given in Eq. (2). Two other doublets with very small intensities also appeared

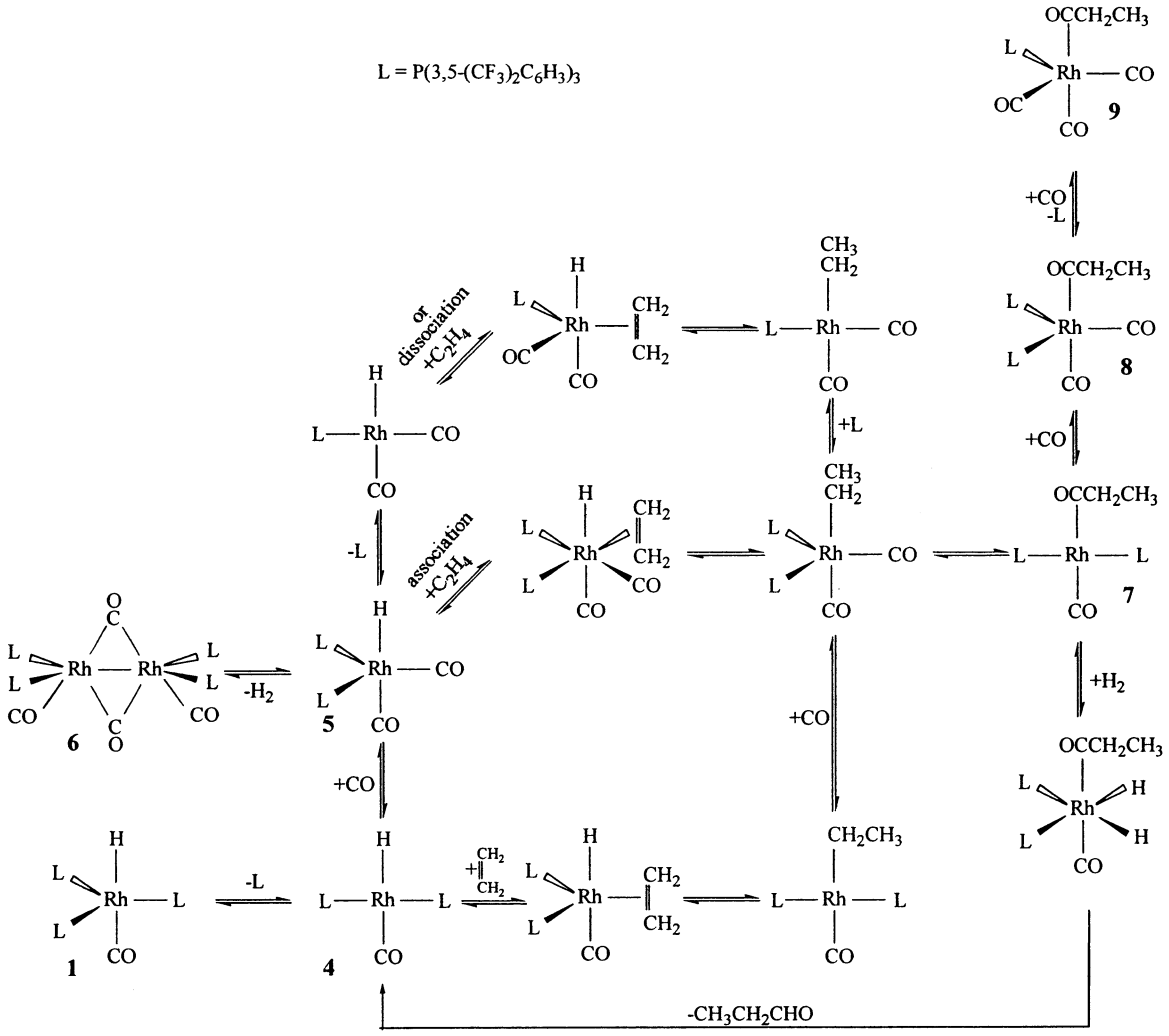

Compound number	Infrared frequencies, cm^{-1}
1	2039, 1952[a] 2041, 1964
4	2066, 2027
5	2076, 2056, 2034
6	1827, 1799[b]
7	1975, 1645
8	2051, 2014, 1673
9	2086, 2033, 2008, 1695

[a] In solid form, the rest of the frequencies are for the compounds in CO_2. [b] Only the bridging carbonyl frequencies are reported here.

Figure 6. Summary of the structure, IR bands, and the reactions of the compounds detected.

on the $^{31}P\{^{1}H\}$ NMR which might be phosphine–metal species.

3. Conclusions

High pressure in situ FTIR spectroscopy was found to be a powerful tool for investigating the effects of ligand modification on the nature of intermediates in hydroformylation of ethylene in supercritical carbon dioxide with $RhH(CO)L_3$ ($L=P(3,5\text{-}(CF_3)_2C_6H_3)_3$). Catalyst concentration for obtaining a satisfactory signal-to-noise ratio was found to be around 2 mM. Marked differences were found between the behavior of $RhH(CO)L_3$ in supercritical carbon dioxide and the $RhH(CO)(PPh_3)_3$ in organic solvents. $RhH(CO)L_3$ does not dissociate in $scCO_2$ and it is converted to $RhH(CO)_2L_2$ and to $[Rh(CO)_2L_2]_2$ in the presence of CO and mainly to $RhH(CO)L_2$ in the presence of an equimolar mixture of CO

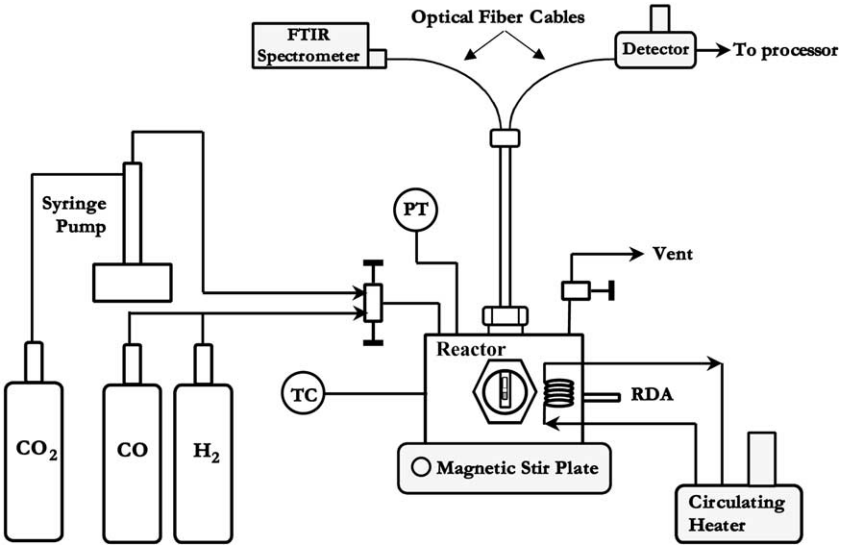

Figure 7. Schematic diagram of the experimental setup.

and H_2. In the presence of CO and C_2H_4, the peaks observed in the acyl region and the terminal metal carbonyl region indicate the formation of three different acylrhodium complexes which are $Rh(CO)L_2(COEt)$, $Rh(CO)_2L_2(COEt)$, and $Rh(CO)_3L(COEt)$. Similar species were also observed during the hydroformylation reaction. A summary of the reactions is shown in Fig. 6 within the framework of the mechanism originally proposed by Wilkinson and co-workers. The IR bands of the observed species are also shown in Fig. 6. The carbonyl stretching frequencies of all of the rhodium–carbonyl species are shifted to higher wavenumbers due to a reduction of electron density at the metal center by the CF_3 groups.

The turnover frequency (TOF) obtained with **1** in $scCO_2$ is about five times higher than the TOF obtained with $RhH(CO)(PPh_3)_3$ in conventional organic solvents at comparable conditions and also about five times higher than the TOF obtained with $RhH(CO)[(4\text{-}F(CF_2)_4\text{-}(CH_2)_3C_6H_4)_3P]_3$ in $scCO_2$.[20] Since the electronic properties of $RhH(CO)(PPh_3)_3$ and $RhH(CO)[(4\text{-}F(CF_2)_4(CH_2)_3\text{-}C_6H_4)_3P]_3$ are similar, the low basicity of the ligand **2** is responsible for the higher activity rather than the effect of the solvent. Based on the spectroscopic measurements presented in this manuscript, the high activity is most likely due to a shift in the equilibrium distribution of the catalytically active intermediates. The species **7** is expected to undergo oxidative addition by hydrogen and the concentration of **7** in solution should be directly proportional to the activity. Since the analog of **7** was never detected under hydroformylation conditions in organic solvents with the conventional catalyst, the higher activity observed is most likely related to the higher concentration of **7** in solution. Furthermore, the decrease in activity with an increase in CO concentration is also related to the equilibria between mono-, di-, and tricarbonyl acyl intermediates. The equilibria are shifted towards the catalytically inactive di- and tricarbonyl acyl rhodium intermediates with increasing CO concentration. Moreover, increasing the CO/H_2 ratio over 1.0 will promote the formation of the inactive dimer species **6**, resulting in a decrease in activity.

4. Experimental

4.1. Experimental apparatus

A schematic diagram of the experimental apparatus is shown in Fig. 7. The set-up consists of a custom manufactured, 51.5 mL stainless steel reactor fitted with two sapphire windows (1″ ID, Sapphire Engineering, Inc.), poly-ether–ether–ketone o-rings (Valco Instruments, Inc.), a T-type thermocouple assembly (Omega Engineering, DP41-TC-MDSS), a pressure transducer (Omega Engineering, PX300-7.5KGV), a vent line, and a rupture disk assembly (Autoclave Engineers). A high-pressure–high temperature FTIR sampling head is screwed through the reactor body to reach inside the reactor. The reactor rests on a magnetic stir plate and is heated to appropriate temperatures by a circulating heater (Fisher Scientific) via a machined internal heating coil. The reactor is pressurized with CO_2 from a syringe pump (ISCO, 260D) equipped with a cooling jacket to the desired reaction pressure.

4.2. Spectra collection

Spectroscopic data are obtained using a Bruker Vector 22 FTIR spectrometer with a Remspec mid-IR fiber optic system comprising a bundle of 19 optical fibers, which transmit in the mid-IR, 5000–900 cm^{-1}. Seven of these fibers are attached to a signal launch module bolted to the collimated external beam port of the spectrometer; 12 fibers are attached to an external, liquid-nitrogen cooled MCT detector provided with specialized optics to optimize capture of the mid-IR signal from the end of the fiber bundle. The combined bundle of 19 fibers is fitted with a high-pressure sampling head. A zinc sulfide optical transfer crystal inside the head transmits the signal into a double-pass, variable-path transmission cell made from stainless steel and returns the signal to the fiber bundle. The sampling head is rated for use at pressures up to 200 bar. IR spectra of solids were measured with the same spectrometer but with internal DTGS detector. The solid sample was grounded into fine particles which was then

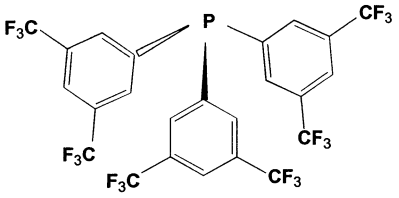

a. The Ligand (L): 3,5-Bis(trifluoromethyl)phenylphosphine **2**.

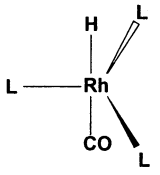

b. The Catalyst: Hydridocarbonyltris(3,5-bis(trifluoromethyl)phenylphosphine)rhodium (I) **1**.

Figure 8. Structure of the ligand and catalyst.

mechanically pressed into a thin wafer. A transparent filler, KBr, was used to give the wafer sufficient mechanical stability and to dilute the solid sample down to 5–10% by weight.

4.3. General procedures

For each experiment, a certain amount of catalyst was placed in the reactor and the vessel was sealed. After acquiring a background spectrum of the empty reactor with optical fibers attached, the vessel was heated or cooled to the desired temperature. Before the system was charged to the desired pressures of the gaseous reactants (CO, H_2, C_2H_4), the reactor was flushed several times with the first added gas. After the system was charged with the gaseous reactants, carbon dioxide was added to the required pressure. Then the IR spectra were acquired as required. Spectral scans were taken at 4 cm^{-1} resolution and signal averaged over 96 or 128 scans, depending on application. No smoothing algorithms were applied to improve visual quality of any spectra presented. To obtain high quality spectra, the carbon dioxide (solvent) spectra or the spectra of a mixture of carbon dioxide and 1:1 mixture of CO/H_2 or only CO at operating conditions and concentrations were subtracted from the spectra of the reaction mixture whenever possible.

4.4. NMR spectra

The ^1H NMR and ^{31}P NMR spectra were acquired at 26°C on a Bruker DRX-400 spectrometer (400.13 and 161.98 MHz, respectively). Chemical shifts are reported in ppm (δ) relative to tetramethylsilane (^1H) or 85% H_3PO_4 (^{31}P).

4.5. Ligand and catalyst preparation

All the chemicals were purchased from Aldrich and used without further purification. First, the fluorinated ligand, 3,5-bis(trifluoromethyl)phenylphosphine (**2**), was prepared using a procedure similar to that described by Bhattacharyya et al.[31] Six grams of 3,5-bis (trifluoromethyl)bromobenzene and 50 cm^3 of diethyl ether were put in a three-necked round-bottom flask. An addition funnel containing 25 cm^3 of diethyl ether was connected to the flask. The flask was placed in dry ice–acetone bath (around −78°C) and flushed with nitrogen. 1.31 g of *n*-butyllithium (1.6 M solution in hexanes) was injected to the addition funnel and the solution was added dropwise to the flask over 1 h and stirred for a further 1 h. A solution of 1.03 g of phosphorus trichloride (10% excess) in 25 ml of diethyl ether was added dropwise, through the addition funnel, to the reaction mixture at −78°C over a further hour. The reaction mixture was then allowed to warm slowly to room temperature with continuous stirring over 12 h. The mixture was hydrolyzed with 25 ml of 10% ammonium chloride aqueous solution. The organic phase was collected and washed twice with water (around 2×25 ml). The organic phase was purified by vacuum distillation. The condensate was collected as a white crystalline product with a yield of 75%. ^1H NMR in acetone-d_6 δ 8.17 (s, 1H), δ 8.21 (d, J(PH)=6.8 Hz, 2H). $^{31}P\{^1H\}$ NMR in acetone-d_6 δ −0.44 (s).

0.093 g (0.36 mmol) of dicarbonylacetylacetonato rhodium (I), $(CO)_2Rh(acac)$, and 1.21 g (1.81 mmol) of **2**, were placed in the high-pressure reactor. After the temperature was raised to 50°C, the reactor was pressurized with a 1:1 mixture of CO/H_2 to 8 bar. Carbon dioxide was pumped in until a pressure of 140 bar was reached. After 45 min, the reactor was cooled down and the $CO_2/CO/H_2$ mixture was slowly vented. The products were collected and washed with chloroform to yield a yellow powder of hydridocarbonyltris(3,5-bis(trifluoromethyl)phenylphosphine)rhodium(I), $HRh(CO)[P(3,5\text{-}(CF_3)_2C_6H_3)_3]_3$ (**1**), (0.44 g, 57%). ^1H NMR in acetone-d_6 δ −9.58 (q, J(RhH)=13.32 Hz, 1H), δ 8.01 (s, 18H), δ 8.19 (s, 9H). $^{31}P\{^1H\}$ NMR in acetone-d_6 δ 47.00 (d, J(PRh)=157.1 Hz). The structures of the ligand **2** and the catalyst **1** are shown in Fig. 8.

Acknowledgements

The authors gratefully acknowledge financial support from the National Science Foundation, Grant# CTS-0080823. The authors also thank the School of Engineering at the University of Connecticut for a generous grant to purchase the FTIR unit.

References

1. Erkey, C. In *Supercritical Fluids Technology in Materials Science and Engineering*; Sun, Y.-P., Ed.; Marcel Dekker: New York, 2002; pp 189–226.
2. Jessop, P.; Ikariya, T.; Noyori, R. *Chem. Rev.* **1999**, *99*, 475–493.
3. Tsang, C.; Street, W. *Chem. Engng Sci.* **1981**, *36*, 993–999.
4. Palo, D. R.; Erkey, C. *J. Chem. Engng Data* **1998**, *43*, 47–49.
5. Laintz, K.; Wai, C.; Yonker, C.; Smith, R. *J. Supercrit. Fluids* **1991**, *4*, 194–198.
6. DeSimone, J.; Maury, E.; Menceloglu, Y.; Combes, J.; McClain, J.; Romack, T. *Science* **1994**, *65*, 356–359.
7. Yazdi, A. V.; Beckman, E. *Ind. Engng Chem. Res.* **1996**, *35*, 3644–3652.
8. Kainz, S.; Koch, D.; Baumann, W.; Leitner, W. *Angew. Chem., Int. Ed. Engl.* **1997**, *36*, 1628–1629.
9. Horvath, I. T.; Rabai, J. *Science* **1994**, *266*, 72–75.
10. Horvath, I.; Kiss, G.; Cook, R. A.; Bond, J.; Stevens, P.; Rabai, J.; Mozeleski, E. *J. Am. Chem. Soc.* **1998**, *120*, 3133–3143.
11. Juliette, J. J. J.; Horvath, I. T.; Gladysz, J. *Angew. Chem., Int. Ed. Engl.* **1997**, *36*, 1610–1612.
12. Sinou, D.; Pozzi, G.; Hope, E. G.; Stuart, A. M. *Tetrahedron Lett.* **1999**, *40*, 849–852.
13. Hamilton, D. J.; Payne, M. J. *Chem. Commun.* **1997**, 1127–1130.
14. Fawcett, J.; Hope, E. G.; Kemmitt, R. D. W. P.; Russell, D. R.; Stuart, A. M. *J. Chem. Soc., Dalton Trans.* **1998**, 3751–3763.
15. Davis, T.; Erkey, C. *Ind. Engng Chem. Res.* **2000**, *39*, 3671–3678.
16. Palo, D. R.; Erkey, C. *Ind. Engng Chem. Res.* **1999**, *38*, 3786–3792.
17. Kainz, S.; Brinkmann, A.; Leitner, W.; Pfaltz, A. *J. Am. Chem. Soc.* **1999**, *121*, 6421–6429.
18. Wegner, A.; Leitner, W. *Chem. Commun.* **1999**, 1583–1584.
19. Francio, G.; Leitner, W. *Chem. Commun.* **1999**, 1663–1664.
20. Palo, D. R.; Erkey, C. *Organometallic* **2000**, *19*, 81–86.
21. Evans, D.; Wilkinson, G. *J. Chem. Soc. (A)* **1968**, 2660–2665.
22. Evans, D.; Osborn, J. A.; Wilkinson, G. *J. Chem. Soc. (A)* **1968**, 3133–3142.
23. Yagupsky, G.; Brown, C. K.; Wilkinson, G. *J. Chem. Soc. (A)* **1970**, 1392–1401.
24. Brown, C. K.; Wilkinson, G. *J. Chem. Soc. (A)* **1970**, 2753–2764.
25. Morris, D. E.; Tinker, H. B. *Chemtech* **1972**, 554–559.
26. Moser, W. R.; Berard, J. R.; Melling, P. J.; Burger, R. *J. Appl. Spectrosc.* **1992**, *46*, 1105–1112.
27. Moser, W. R.; Papile, C. J.; Brannon, D. A.; Duwell, R. A.; Weininger, S. J. *J. Mol. Catal.* **1987**, *41*, 271–292.
28. Moser, W. R.; Papile, C. J.; Wieninger, S. J. *J. Mol. Catal.* **1987**, *41*, 293–302.
29. Buback, M. *Angew. Chem., Int. Ed. Engl.* **1991**, *30*, 641–653.
30. Bianchini, C.; Lee, H. M.; Meli, A.; Vizza, F. *Organometallics* **2000**, *19*, 839–843.
31. Bhattacharyya, P.; Gudmunsen, D.; Hop, E. G.; Kemmitt, R. D. W.; Paige, D. R.; Alison, M. *J. Chem. Soc., Perkin Trans. 1* **1997**, 3609–3612.